ISSN 1392-1207. MECHANIKA. Vol. 30, No. 6, 2024: 568–575

Calculation Method of Complete Dynamic Characteristics Coefficients for Tilting Pad Bearings Based on Equivalent Motion of Babbitt Pads

Xiaoming SONG*, Yingjuan DONG, Tao BAI***, Jianguo YU******

**Department of Mechanical Engineering, Hebei Petroleum University of Technology, Chengde067000, China, E-mail: songxm012@126.com*

***Department of Mechanical Engineering, Hebei Petroleum University of Technology, Chengde067000, China, E-mail: cdkfq167@163.com (Corresponding author)*

****Department of Mechanical Engineering, Hebei Petroleum University of Technology, Chengde067000, China, E-mail: wanglei19880309@163.com*

*****Department of Mechanical Engineering, Hebei Petroleum University of Technology, Chengde067000, China, E-mail: jianguo_yu2024@163.com*

https://doi.org/10.5755/j02.mech.38127

1. Introduction

Tilting-pad bearings, due to their high stability, are widely utilized in various occasions [1-4]. Compared to fixed-pad sliding bearings, the dynamic characteristics of tilting-pad bearings are not only related to the dynamic properties of the oil film but also influenced by the pad tilting motion. In essence, the dynamic behavior of tilting-pad bearings is a comprehensive reflection of both the dynamic coefficient of the oil film and the tilting motion of the pads [5]. Precise determination of the tilting-pad bearings dynamic characteristic coefficients holds significant importance for elucidating their dynamic behaviors and devising strategies to mitigate vibrations and noise. Furthermore, this constitutes a vital step towards achieving effective vibration fault diagnosis [6].

Lund [7] proposed the use of eight dynamic coefficients to characterize the dynamic behavior of tilting-pad bearings, a method that shares similarities with the eight coefficients used to describe the dynamic characteristics of fixed-pad bearings. These eight dynamic coefficients are easy to understand and convenient for engineering applications, and they are still widely adopted in the industry today [8,9]. However, as energy equipment continues to evolve towards higher rotational speeds and larger capacities, the instability issues of tilting-pad bearings have become increasingly prominent, drawing attention to the study of their stability. Stability analysis of rotor systems, traditionally conducted with eight dynamic coefficients, frequently results in an oversimplified portrayal of absolute stability, a finding that often fails to reflect real-world scenarios [10, 11]. From the perspectives of degrees of freedom and dynamics, Rouch [12] and Ettles [13] proposed an analytical method that considers the complete set of dynamic coefficients, incorporating pad motion, to describe the dynamic behavior of both the journal and the pads. In the case where the rotor is axially aligned with the pads, the complete set of dynamic coefficients comprises 5n+4 stiffness coefficients and 5n+4 damping coefficients (where n represents the number of pads in the tilting-pad bearing). Using this approach to analyze the stability of the bearing-rotor system comprehensively considers instability factors such as pad inertia, pivot friction, and elastic deformation of the pivot point, leading to more accurate stability analysis results. Works [14, 15] provide the complete set of dynamic coefficients for tilting-pad bearings, particularly the definitions of cross-coupling terms, and presents these dynamic coefficients in matrix form, known as the complete dynamic coefficient matrix.

Based on the definition of the complete set of dynamic coefficients, the pad perturbation method, as proposed in [16], can conveniently calculate the complete dynamic coefficient matrix for tilting-pad bearings. Wang Liping [17] introduced a mathematical analytical model for computing the complete dynamic coefficients of tilting-pad bearings based on the perturbation characteristics of the pads. In [18], the tile perturbation method for calculating the complete dynamic characteristic coefficient of tilting pad bearing is proposed, and the numerical solution is given. Zhang Zhenshan [19] used the complete set of dynamic coefficients to investigate the influence of whirl on the dynamic characteristics, arguing that its effect should not be overlooked. L.E. Barrett et al. [20] examined the eigenvalue dependency of the reduced dynamic coefficients. Other researchers continue to expand the range of factors considered in the calculation of dynamic characteristics of tilting pad bearings and other methods, for example, some researchers have studied the influence of temperature, deformation, pre-load and fulcrum friction on the dynamic characteristics of tilting pad bearings [21, 22]. Yan Zhiyong [21, 23] calculated the complete dynamic coefficients of tilting-pad bearings and applied them to the critical speed calculations of the bearing-rotor system. He also studied the complete dynamic coefficients of tilting-pad bearings considering the elasticity of the pivot points.

To encapsulate, a plethora of research, spanning from national to international realms, has delved into the comprehensive dynamic coefficients of tilting-pad bearings, encompassing a myriad of facets. However, due to the large number of coefficients involved, existing methods are complex and inefficient, which is not conducive to engineering applications.

This paper proposes a calculation method for the complete dynamic coefficients of tilting-pad bearings based on the equivalent motion of the pads. By equivalently treating the pad tilting as journal displacement, the relationship between various parameters of the dynamic coefficients (including stiffness and damping coefficients) is established, thereby simplifying the calculation of the complete dynamic coefficients. This method is applied to calculate the dynamic coefficients of each pad in a 6-pad tilting-pad bearing for a steam turbine. The static equilibrium position of the bearing under a given load condition is iteratively calculated using the eccentricity method, and the variation patterns of the coefficients are identified, verifying the practicality of the proposed method.

2. Complete Dynamic Characteristic of Tilting Pad Bearing

The tilting-pad bearing typically consists of 3 to 6 or even more arcuate pads that can tilt freely on pivot points, as illustrated in Fig. 1. Due to the ability of its pads to swing freely in response to changes in rotational speed, load, and bearing temperature, multiple oil wedges are formed around the journal. Furthermore, the pressure of each oil film always directs towards the center (a). Therefore, the tilting-pad bearing exhibits high stability.

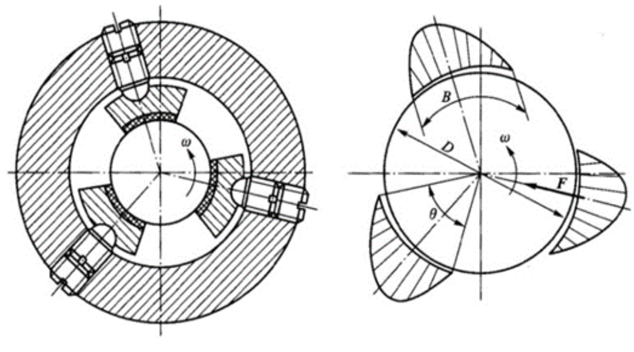

a b

Fig. 1 Structural schematic diagram of tilting pad bearing: a – profile of tilting pad bearing, b – arrangement of pads and hydrodynamic pressure profiles

In large-scale machinery, the pivot points of the tilting pads are often designed in a spherical form. It can be assumed that the journal and the pads maintain parallelism in the axial direction, with the pads swinging around the pivot points. Due to the increased freedom of movement in the pads' tilting, the complete dynamic characteristic coefficients of the tilting-pad bearing require a larger number of coefficients to represent the bearing's properties. Additionally, the number of required coefficients varies depending on the number of bearing pads.

As shown in Fig. 2, the components F_{xi} and F_{yi} of the oil film force of tilting tile in the x and y directions, as well as the moment M_i around the fulcrum, can be expressed as functions of the journal position (x, y), speed

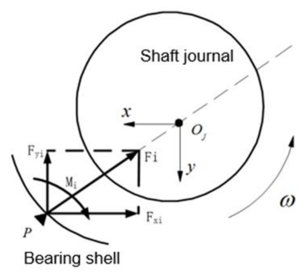

Fig. 2 Oil film force and torque of tile

$(\dot{x}, \dot{y})$ and the swing angle and speed $(\varphi_i, \dot{\varphi}_i)$ of the tile, as shown in Eq. (1)

$$\begin{cases} F_{xi} = f_x\left(x, y, \dot{x}, \dot{y}, \varphi_i, \dot{\varphi}_i\right), \\ F_{yi} = f_y\left(x, y, \dot{x}, \dot{y}, \varphi_i, \dot{\varphi}_i\right), . \\ M_i = m\left(x, y, \dot{x}, \dot{y}, \varphi_i, \dot{\varphi}_i\right). \end{cases} \tag{1}$$

Balance tile position $s_0 = \{x_0, y_0, \dot{x}_0, \dot{y}_0, \varphi_{i0}, \dot{\varphi}_{i0}\}$, by performing the Taylor expansion of Eq. (1) at s_0, while ignoring the higher order terms, then F_{xi} , F_{yi} and M_i can be expressed as:

$$\begin{cases} F_{xi} = F_{xi}\left(s_0\right) + k_{xxi}x + c_{xxi}\dot{x} + \\ \quad + k_{xyi}y + c_{xyi}\dot{y} + k_{x\varphi i}\varphi_i + c_{x\varphi i}\dot{\varphi}_i, \\ F_{yi} = F_{yi}\left(s_0\right) + k_{yxi}x + c_{yxi}\dot{x} + \\ \quad + k_{yyi}y + c_{yyi}\dot{y} + k_{y\varphi i}\varphi_i + c_{y\varphi i}\dot{\varphi}_i, \\ M_i = M_i\left(s_0\right) + k_{\varphi xi}x + c_{\varphi xi}\dot{x} + \\ \quad + k_{\varphi yi}y + c_{\varphi yi}\dot{y} + k_{\varphi\varphi i}\varphi_i + c_{\varphi\varphi i}\dot{\varphi}_i. \end{cases} \tag{2}$$

where $k_{xxi} = \left.\frac{\partial F_{xi}}{\partial x}\right|_{s_0}$, $k_{xyi} = \left.\frac{\partial F_{xi}}{\partial y}\right|_{s_0}$, $k_{yyi} = \left.\frac{\partial F_{yi}}{\partial y}\right|_{s_0}$, $k_{yxi} = \left.\frac{\partial F_{yi}}{\partial x}\right|_{s_0}$, $k_{x\varphi i} = \left.\frac{\partial F_{xi}}{\partial \varphi_i}\right|_{s_0}$, $k_{y\varphi i} = \left.\frac{\partial F_{yi}}{\partial \varphi_i}\right|_{s_0}$, $c_{xxi} = \left.\frac{\partial F_{xi}}{\partial \dot{x}}\right|_{s_0}$, $c_{xyi} = \left.\frac{\partial F_{xi}}{\partial \dot{y}}\right|_{s_0}$, $c_{yyi} = \left.\frac{\partial F_{yi}}{\partial \dot{y}}\right|_{s_0}$, $c_{yxi} = \left.\frac{\partial F_{yi}}{\partial \dot{x}}\right|_{s_0}$, $c_{x\varphi i} = \left.\frac{\partial F_{xi}}{\partial \dot{\varphi}_i}\right|_{s_0}$, $c_{y\varphi i} = \left.\frac{\partial F_{yi}}{\partial \dot{\varphi}_i}\right|_{s_0}$, $k_{\varphi xi} = \left.\frac{\partial M_i}{\partial x}\right|_{s_0}$, $k_{\varphi yi} = \left.\frac{\partial M_i}{\partial y}\right|_{s_0}$, $k_{\varphi\varphi i} = \left.\frac{\partial M_i}{\partial \varphi_i}\right|_{s_0}$, $c_{\varphi xi} = \left.\frac{\partial M_i}{\partial \dot{x}}\right|_{s_0}$, $c_{\varphi yi} = \left.\frac{\partial M_i}{\partial \dot{y}}\right|_{s_0}$, $c_{\varphi\varphi i} = \left.\frac{\partial M_i}{\partial \dot{\varphi}_i}\right|_{s_0}$.

The coefficients related to the oil film force can be calculated using Eq. (3)

$$\begin{cases} k_{xx} = \sum_{i=1}^{n} k_{xxi},\ k_{xy} = \sum_{i=1}^{n} k_{xyi},\ k_{yx} = \sum_{i=1}^{n} k_{yxi},\ k_{yy} = \sum_{i=1}^{n} k_{yyi}, \\ c_{xx} = \sum_{i=1}^{n} c_{xxi},\ c_{xy} = \sum_{i=1}^{n} c_{xyi},\ c_{yx} = \sum_{i=1}^{n} c_{yxi},\ c_{yy} = \sum_{i=1}^{n} c_{yyi}. \end{cases} \tag{3}$$

3. Computation Method of Complete Dynamic Characteristic Coefficients

Through the definition of the complete dynamic characteristic coefficient, it can be seen that 18n dynamic characteristic coefficients k_{xxi}, k_{xyi}, k_{yxi}, k_{yyi}, $k_{x\varphi i}$, $k_{\varphi xi}$, $k_{y\varphi i}$, $k_{\varphi yi}$, $k_{\varphi\varphi i}$, c_{xxi}, c_{xyi}, c_{yxi}, c_{yyi}, $c_{x\varphi i}$, $c_{\varphi xi}$, $c_{y\varphi i}$, $c_{\varphi yi}$, $c_{\varphi\varphi i}$ need to be calculated first to calculate the complete dynamic characteristic coefficient of bearings. Due to the excessive number of coefficients, if the calculation is carried out directly, the workload is large and the calculation is complicated, which is not conducive to engineering application.

In order to solve the above problems, this paper introduces the geometric relationship between tile swing and journal disturbance to simplify the above equations, and reduces the 18n coefficients required to be calculated to 8n, such as k_{xxi}, k_{xyi}, k_{yxi}, k_{yyi}, c_{xxi}, c_{xyi}, c_{yxi}, c_{yyi}, which greatly reduces the calculation workload and improves the calculation efficiency and stability. These 8n coefficients can be obtained by treating the tile as fixed and applying displacement or velocity perturbations to the journal.

A coordinate system for calculating the performance of the tilting-pad bearing, as depicted in Fig. 3, is established. When the pad tilts from its static equilibrium position by an angle φ_i to a new position, the center of the pad arc moves from O_p to O'_p. From the perspective of the coordinate system $x'o_py'$ fixed at O_p and swinging along with the pad, the journal moves in the opposite direction to a new position O'_j. Using a similar approach, the angular velocity of the tilt can be equivalently represented as the displacement velocity of the journal. Based on this transformation concept, the tilting of the pad is equivalent to the movement of the journal, and the transformation relationship is as follows:

$$\begin{cases} x_i = r\varphi_i \cos(\pi - \beta_i), \\ y_i = -r\varphi_i \sin(\pi - \beta_i), \\ \dot{x}_i = r\dot{\varphi}_i \cos(\pi - \beta_i), \\ \dot{y}_i = -r\dot{\varphi}_i \sin(\pi - \beta_i). \end{cases} \tag{4}$$

In Eq. (4), φ_i is the tile swing angle; r is the radius of the tile surface arc; β_i is the circumferential position angle of tile fulcrum.

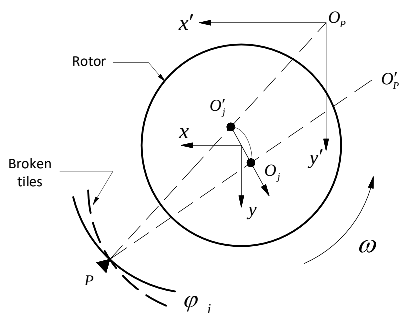

Fig. 3 Coordinate system for calculation of tile performance

The components of the oil film force of a single tilting tile in the x and y directions are F_{xi} and F_{yi}, respectively. The derivatives of the oil film forces F_{xi}, and F_{yi} with respect to the swing angle of the tile φ_i and the derivatives of the oil film forces with respect to the journal displacement x_i and y_i are:

$$\begin{cases} \dfrac{\partial F_{xi}}{\partial \varphi_i} = \dfrac{\partial F_{xi}}{\partial x_i} \cdot \dfrac{\partial x_i}{\partial \varphi_i} + \dfrac{\partial F_{xi}}{\partial y_i} \cdot \dfrac{\partial y_i}{\partial \varphi_i}, \\ \dfrac{\partial F_{yi}}{\partial \varphi_i} = \dfrac{\partial F_{yi}}{\partial x_i} \cdot \dfrac{\partial x_i}{\partial \varphi_i} + \dfrac{\partial F_{yi}}{\partial y_i} \cdot \dfrac{\partial y_i}{\partial \varphi_i}. \end{cases} \tag{5}$$

From Eq. (5), it follows that

$$\begin{cases} \dfrac{\partial F_{xi}}{\partial \varphi_i} = r\cos(\pi - \beta_i)\dfrac{\partial F_{xi}}{\partial x_i} - r\sin(\pi - \beta_i)\dfrac{\partial F_{xi}}{\partial y_i}, \\ \dfrac{\partial F_{yi}}{\partial \varphi_i} = r\cos(\pi - \beta_i)\dfrac{\partial F_{yi}}{\partial x_i} - r\sin(\pi - \beta_i)\dfrac{\partial F_{yi}}{\partial y_i}. \end{cases} \tag{6}$$

The solution of the moment M_i of the tile around the fulcrum can be converted into the solution of the oil film force F_{xi} and F_{yi}, and then M_i is obtained by using these two oil film force data. The transformation relation between M_i, F_{xi} and F_{yi} is:

$$M_i = F_{yi} \cdot r\sin\beta_i - F_{xi} \cdot r\cos\beta_i. \tag{7}$$

The derivatives of M_i, with respect to x_i, y_i and φ_i, F_{xi} and F_{yi}, with respect to the displacement of the journal x_i and y_i, also have a certain relationship, which can be obtained by substitutions and other methods in the derivation of multivariate functions. The specific relationship and its derivation are as follows:

$$\begin{cases} \dfrac{\partial M_i}{\partial x_i} = \dfrac{\partial F_{yi}}{\partial x_i} r\sin\beta_i - \dfrac{\partial F_{xi}}{\partial x_i} r\cos\beta_i, \\ \dfrac{\partial M_i}{\partial y_i} = \dfrac{\partial F_{yi}}{\partial y_i} r\sin\beta_i - \dfrac{\partial F_{xi}}{\partial y_i} r\cos\beta_i, \\ \dfrac{\partial M_i}{\partial \varphi_i} = \dfrac{\partial F_{yi}}{\partial x_i} r^2\cos(\pi - \beta_i)\sin\beta_i - \\ \quad -\dfrac{\partial F_{yi}}{\partial y_i} r^2\sin(\pi - \beta_i)\sin\beta_i - \\ \quad -\dfrac{\partial F_{xi}}{\partial x_i} r^2\cos(\pi - \beta_i)\cos\beta_i + \\ \quad +\dfrac{\partial F_{xi}}{\partial y_i} r^2\sin(\pi - \beta_i)\cos\beta_i. \end{cases} \tag{8}$$

The derivatives in Eq. (6) and Eq. (8) are taken at the equilibrium position of the tile and the journal, then the relationship between the stiffness coefficients of the oil film can be obtained:

$$\begin{cases} k_{x\varphi i} = r\cos(\pi - \beta_i)k_{xxi} - r\sin(\pi - \beta_i)k_{xyi}, \\ k_{y\varphi i} = r\cos(\pi - \beta_i)k_{yxi} - r\sin(\pi - \beta_i)k_{yyi}, \\ k_{\varphi xi} = k_{yxi} r\sin\beta_i - k_{xxi} r\cos\beta_i, \\ k_{\varphi yi} = k_{yyi} r\sin\beta_i - k_{xyi} r\cos\beta_i, \\ k_{\varphi\varphi i} = k_{yxi} r^2\cos(\pi - \beta_i)\sin\beta_i - \\ \quad -k_{yyi} r^2\sin(\pi - \beta_i)\sin\beta_i - \\ \quad -k_{xxi} r^2\cos(\pi - \beta_i)\cos\beta_i + \\ \quad +k_{xyi} r^2\sin(\pi - \beta_i)\cos\beta_i. \end{cases} \tag{9}$$

It can be seen from Eq. (9) that the 5n stiffness coefficients can be represented by another 4n coefficients.

Similarly, the damping coefficient has a similar relationship with the stiffness, as shown in Eq. (10).

$$\begin{cases} c_{x\varphi i} = r\cos(\pi - \beta_i)c_{xxi} - r\sin(\pi - \beta_i)c_{xyi}, \\ c_{y\varphi i} = r\cos(\pi - \beta_i)c_{yxi} - r\sin(\pi - \beta_i)c_{yyi}, \\ c_{\varphi xi} = c_{yxi} r\sin\beta_i - c_{xxi} r\cos\beta_i, \\ c_{\varphi yi} = c_{yyi} r\sin\beta_i - c_{xyi} r\cos\beta_i, \\ c_{\varphi\varphi i} = c_{yxi} r^2\cos(\pi - \beta_i)\sin\beta_i - \\ \quad -c_{yyi} r^2\sin(\pi - \beta_i)\sin\beta_i - \\ \quad -c_{xxi} r^2\cos(\pi - \beta_i)\cos\beta_i + \\ \quad +c_{xyi} r^2\sin(\pi - \beta_i)\cos\beta_i. \end{cases} \tag{10}$$

Based on the aforementioned relationships, the eight coefficients for a single pad can be calculated using the same method as for fixed-pad bearings. Subsequently, the complete dynamic characteristic coefficients can be derived using the above equations, without the need for additional calculations involving angular perturbations to obtain the relevant coefficients. This approach is similar to the method used for solving dynamic characteristic coefficients in fixed-pad bearings, significantly reducing the number of calculations required for the Reynolds equation, effectively improving computational efficiency, and facilitating understanding and application by engineering personnel.

4. Simulation Example

In this paper, a six-pad tilting-pad bearing used in a steam turbine set is taken as the application object, as shown in Fig. 4. This research object exhibits geometric symmetry, and its specific parameters are listed in Table 1.

In general, the static equilibrium position of the bearing is unknown, while the static load is given. Therefore, to calculate the stiffness and damping coefficients of the bearing under a given load condition, it is necessary to first determine the static equilibrium position corresponding to that condition. In this paper, the eccentricity ratio method is adopted to determine the static equilibrium position of the bearing.

Firstly, a mathematical model of the tilting-pad bearing is constructed, which includes the Reynolds equation and the oil film thickness equation. It is assumed that

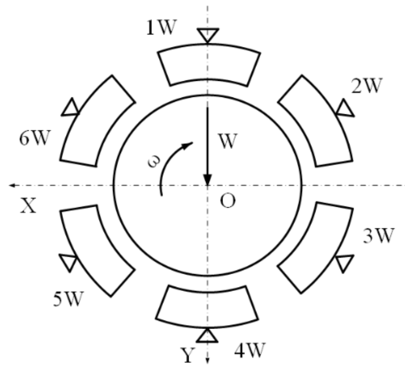

Fig. 4 Bearing structure diagram

the lubricant flow is laminar, and the temperature of the lubricant during stable bearing operation is 70°C. Subsequently, with a given eccentricity ratio of 0.50, the relevant mathematical equations are solved simultaneously using the finite difference method to determine the static equilibrium position of the bearing and calculate the corresponding oil film force and moment.

Table 2 shows the calculation iterative process of determining the static balance position of the bearing at any given initial position (eccentricity is 0.50) under the action of the determined rated load of 240 kN. As can be seen from the table, after more than 9 iterations, it converges to the rated load. At this time, the eccentricity is 0.5658, the deviation Angle is 0.774°, the minimum oil film thickness is 25.64 μm, and the error between the final iteration load and the rated load is 0.01. It can be seen that this method has fast convergence, and higher calculation accuracy can be achieved by selecting the appropriate initial position after few iterative steps.

Table 1

Bearing parameter

Parameter	Diameter *D*, mm	Breadth, mm	Clearance ratio	Feed temperature, °C	Number of tiles	Tilting angle, °	Fulcrum coefficient	Lube	Rated speed, rpm	Load rating, kN
Value	400	300	1.3‰	40	6	56	0.5	VG46	3000	240

Table 2

Iterative process of balance position of six-watt tilting pad bearing

Iterations	Eccentricity ratio	Angle of displacement, °	Load, kN	Flow, L/min	Minimum oil film thickness, μm
0	0.50	1.481	177.33	1190.74	29.67
1	0.5261	1.133	199.09	1209.15	28.08
2	0.5432	0.983	215.18	1212.22	27.01
3	0.5535	0.75	226.14	1214.08	26.39
4	0.5593	0.77	232.20	1215.17	26.03
5	0.5625	0.751	236.10	1215.68	25.82
6	0.5642	0.707	237.77	1216.07	25.74
7	0.5651	0.741	238.87	1216.29	25.66
8	0.5656	0.781	239.48	1216.33	25.64
9	0.5658	0.774	240.01	1215.93	25.64

After locating the static equilibrium position of the bearing, the complete dynamic characteristic coefficients of the bearing are calculated using the method proposed in this paper, and their variation patterns are analyzed. The outcomes of our calculations are delineated in Fig. 5 through 12.

Fig. 5 shows the variation of bearing stiffness with rotational speed. It can be observed that the primary stiffness in the vertical direction (k_{yy}) of the tilting-pad bearing decreases as the rotational speed increases, while the primary stiffness in the horizontal direction (k_{xx}) increases slightly with increasing rotational speed. Fig. 6 illustrates the change in bearing damping with rotational speed. It can be seen that the damping of the tilting-pad bearing decreases as the rotational speed increases, and the cross-damping coefficients c_{xy} and c_{yx} are equal. The patterns of these eight dynamic characteristic coefficients in Figs. 5 and 6 are similar to those of the eight coefficients for fixed-pad bearings.

Fig. 7 and Fig. 8 show the variation diagrams of $k_{x\varphi i}$ and $k_{y\varphi i}$ with load respectively, from which the symmetry of bearings can be seen. The 1, 2 and 6 watts of the 6 watt tilting tile bearing are upper watts, and because the bearing load is very small, $k_{x\varphi i}$ and $k_{y\varphi i}$ are almost 0, so

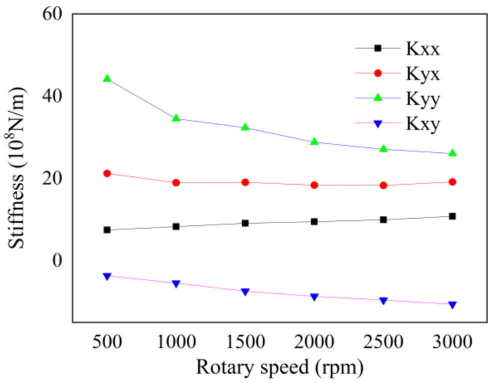

Fig. 5 Stiffness changes with speed

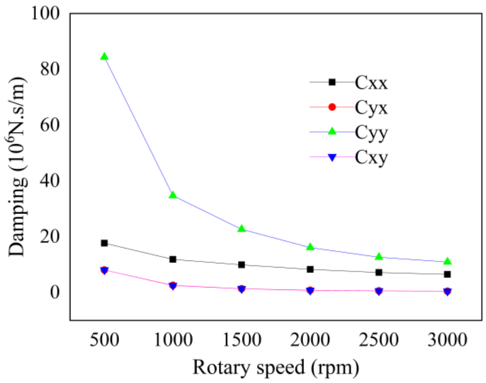

Fig. 6 Damping changes with speed

their swing has little effect on the oil film force in the *x* direction and *y* direction of the bearing. Tile 3 and tile 5 are symmetrically distributed, and their oscillations have roughly similar effects on the oil film force in the *x* direction and *y* direction of the bearing. Considering the influence of the position of the tile, $k_{x\varphi 3} \approx -k_{x\varphi 5}$, $k_{y\varphi 3} \approx k_{y\varphi 5}$.

Fig. 9 shows the variation diagram of $k_{\varphi\varphi i}$ with load. $k_{\varphi\varphi i}$ represents the influence of small amplitude swing of the tile near the equilibrium position on the oil film torque of the tile, in unit N·m/rad. Because the 1 watt, 2 watt and 6 watts of the 6 watt tilting tile bearing do not bear load, the oil film force and moment on the tile surface are almost 0, so the swing of the tile has little effect on the moment on the tile. Tile 3 and tile 5 are distributed symmetrically, and the oil film force on the tile is roughly the same, so $k_{\varphi\varphi 3} \approx k_{\varphi\varphi 5}$.

Fig. 10 and Fig. 11 represent the influence of small movements of the journal in the x and y directions

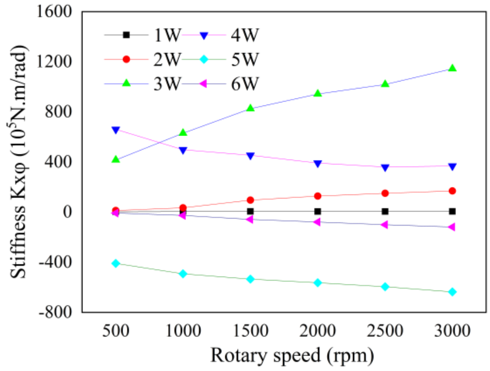

Fig. 7 Variation of $k_{x\varphi i}$ with speed

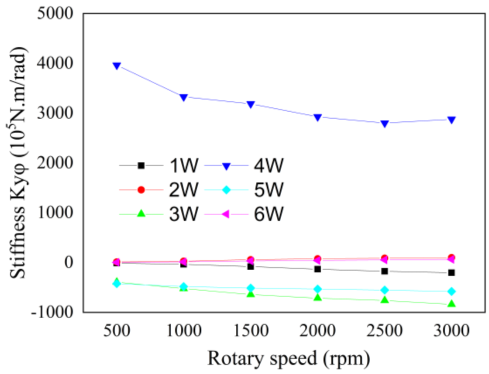

Fig. 8 Variation of $k_{y\varphi i}$ with speed

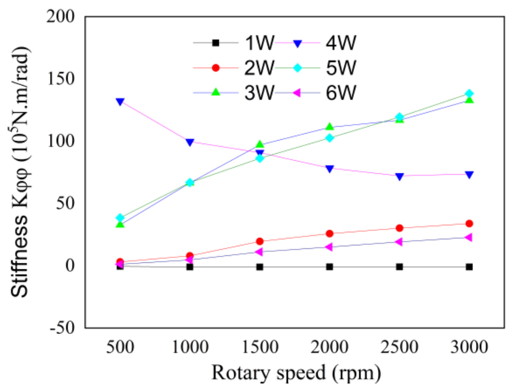

Fig. 9 Variation of $k_{\varphi\varphi i}$ with speed

centered on the balance position on the tile torque. Due to the symmetry of the 6-watt tilting tile bearing, the curve in Fig. 10 is symmetrical distribution, and the figure is $k_{\varphi x3} \approx -k_{\varphi x5}$, $k_{\varphi x2} \approx -k_{\varphi x6}$. Tile 1 is not load-bearing, $k_{x\varphi 1} = 0$, and the influence of the small movement of the journal on the moment on tile 1 is 0. At the same time, $k_{x\varphi 1} = 0$. Compared with other tiles, the small movement in the y direction of the journal has the greatest influence on the torque of the 4-tile.

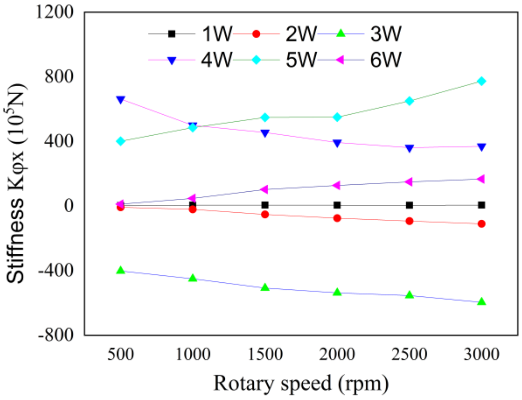

Fig. 10 Variation of $k_{\varphi xi}$ with speed

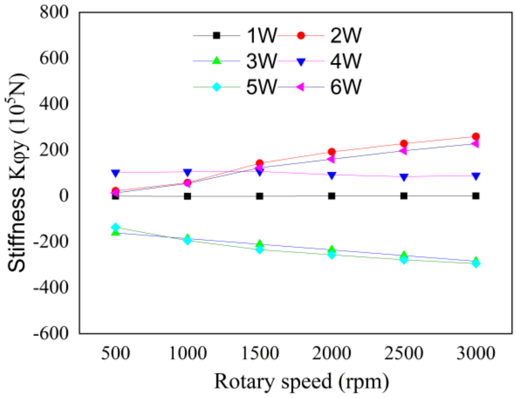

Fig. 11 Variation of $k_{\varphi yi}$ with speed

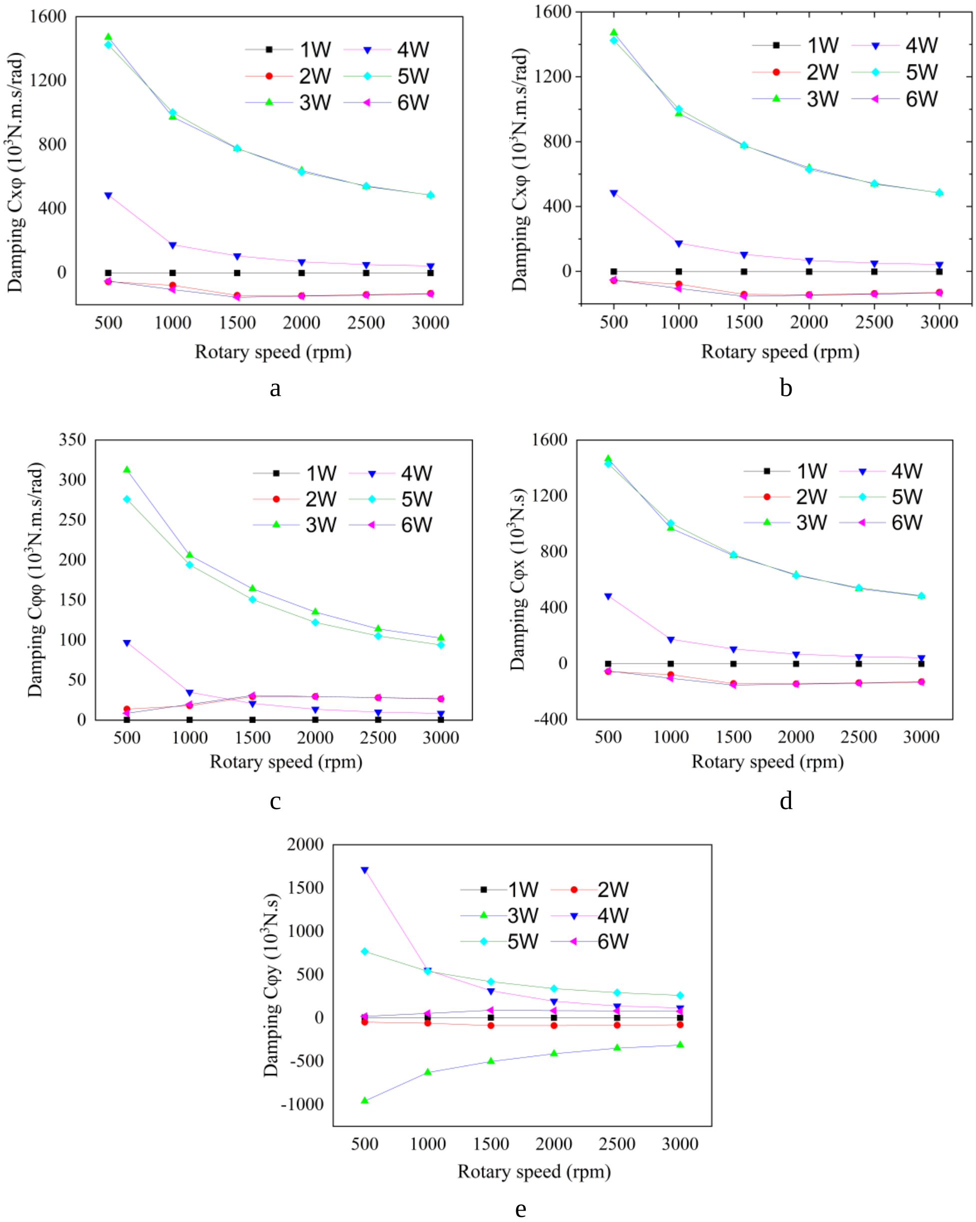

Fig. 12 Damping changes with speed: a – $c_{x\varphi i}$ varies with the speed, b – $c_{y\varphi i}$ varies with the speed, c – $c_{\varphi\varphi i}$ varies with the speed, d – $c_{\varphi xi}$ varies with speed, e – $c_{\varphi yi}$ varies with speed

The variation law of damping coefficient with speed is roughly consistent with that of stiffness, which can reflect the damping condition of specific tiles, as shown in Fig. 12. The law is not to be repeated.

It can be seen from the above analysis that the bearing stiffness coefficient and damping coefficient obtained by solving the complete dynamic characteristic coefficient of tilting tile bearings based on tile motion equivalence are almost 0 on non-bearing tiles, and they are roughly the same on symmetrical bearing tiles, and their variation rules are consistent with bearing structure and stress conditions. Compared with the tile disturbance method, this method is convenient and fast, and the results can accurately describe the motion state of each tile.

5. Conclusions

1. Based on the motion equivalence of tile, a method for solving the complete dynamic characteristic coefficient of tilting tile bearing is proposed. Compared with the tile disturbance method, this method can effectively reduce the solving times of Reynolds equation and improve the computational efficiency and stability. From the point of view of application, this method is easy to calculate, simple, easy to accept and understand, so it has more advantages.

2. The calculation example of the complete dynamic characteristic coefficient based on the motion equivalence of tiles shows that the relationship between the relevant dynamic coefficients of different tiles is consistent with the bearing structure and stress conditions: the law of 8 dynamic characteristic coefficients (k_{xx}, k_{yy}, k_{xy}, k_{yx}, c_{xx}, c_{yy}, c_{xy}, c_{yx}) is similar to the law of 8 coefficients of the dynamic characteristic of fixed tile bearings; Bearing or tile disturbance has little effect on oil film force or oil film moment, and its dynamic characteristic coefficient is close to 0. The bearing or tile disturbance has a great influence on the oil film force or oil film moment related to the bearing tile, which is also obviously reflected in the dynamic characteristic coefficient. The calculation results verify the practicability of the method.

References

1. **Rendl, J.; Dyk, Š.; Smolík, L.** 2021. Nonlinear dynamic analysis of a tilting pad journal bearing subjected to pad fluttering, Nonlinear Dynamics 105: 2133-2156. https://doi.org/10.1007/s11071-021-06748-x.
2. **Benti, G. B.; Gustavsson, R.; Aidanpää, J. O.** 2022. Speed-Dependent Bearing Models for Dynamic Simulations of Vertical Rotors, Machines 10(7): 556. https://doi.org/10.3390/machines10070556.
3. **Liu, B., Zhao, W., Bai, S., Hu, B., Wu, K., Zhao, Q.** 2023. The effect of misalignment on the performance of tilting pad thrust bearing with TEHD coupling model and turbulence model, Advances in Mechanical Engineering 15(6): 16878132231176191. https://doi.org/10.1177/16878132231176191.
4. **Rondon, D., Benti, G. B., Aidanpää, J. O., Gustavsson, R.** 2022. Rotordynamic Characterization of Tilting-Pad Bearings with Eight Pads in Vertical Rotors, ASME Journal of Energy Resources Technology 144(1): 012111. https://doi.org/10.1115/1.4051803.
5. **Colmenares, L. E. R.** 2004. Experimental frequency-dependent rotordynamic coefficients for a load-on-pad, high-speed, flexible-pivot tilting-pad bearing. Texas A&M University. 64p. Available at: https://hdl.handle.net/1969.1/138.
6. **Ouyang, W.; Liu, Q.; Cheng, Q.; Wan, G.; Jin, Y.** 2022. Identification of Distributed Dynamic Characteristics of Journal Bearing with Large Aspect Ratio under Shaft Bending, Journal of Marine Science and Engineering 10(5): 658. https://doi.org/10.3390/jmse10050658.
7. **Lund, J. W.** 1964. Spring and Damping Coefficients for the Tilting-Pad Journal Bearing, Tribology Transactions 7(4): 342-352. https://doi.org/10.1080/05698196408972064.
8. **Tiwari, R.; Lees, A. W.; Friswell, M. I.** 2004. Identification of Dynamic Bearing Parameters: A Review, The Shock and Vibration Digest 36(2): 99-124. https://doi.org/10.1177/0583102404040173.
9. **Dang, P. V.; Chatterton, S.; Pennacchi, P.; Vania, A.** 2016. Effect of the load direction on non-nominal five-pad tilting-pad journal bearings, Tribology International 98: 197-211. https://doi.org/10.1016/j.triboint.2016.02.028.
10. **Athre, K.; Kurian, J.; Gupta, K. N.; Garg, R. D.** 1982. A Numerical Approach to the Stability of Rotor-Bearing Systems, ASME Journal of Mechanical Design 104(2): 356-363. https://doi.org/10.1115/1.3256351.
11. **Wilkes, J. C.; Childs, D. W.** 2012. Tilting Pad Journal Bearings—A Discussion on Stability Calculation, Frequency Dependence, and Pad and Pivot, ASME Journal of Engineering for Gas Turbines and Power 134(12): 122508. https://doi.org/10.1115/1.4007369.
12. **Rouch, K. E.** 1983. Dynamics of Pivoted-Pad Journal Bearings, Including Pad Translation and Rotation Effects, Tribology Transactions 26(1): 102-109. https://doi.org/10.1080/05698198308981483.
13. **Ettles, C. M. M.** 1980. The Analysis and Performance of Pivoted Pad Journal Bearings Considering Thermal and Elastic Effects, ASME Journal of Tribology 102(2): 182-192. https://doi.org/10.1115/1.3251465.
14. **Barrett, L. E.; Allaire, P. E.; Wilson, B. E.** 1988. The Eigenvalue Dependence of Reduced Tilting Pad Bearing Stiffness and Damping Coefficients, Tribology Transactions 31(4): 411-419. https://doi.org/10.1080/10402008808981842.
15. **Suh, J.; Palazzolo, A.** 2015. Three-Dimensional Dynamic Model of TEHD Tilting-Pad Journal Bearing—Part II: Parametric Studies, ASME Journal of Tribology 137(4): 041704. https://doi.org/10.1115/1.4030021.
16. **Hagemann, T.; Schwarze, H.** 2015. A Theoretical Study on Frequency Effects on Tilting-Pad Journal Bearing Dynamic Coefficients, In: Pennacchi, P. (eds) Proceedings of the 9th IFToMM International Conference on Rotor Dynamics, Mechanisms and Machine Science 21: 1069-1080. https://doi.org/10.1007/978-3-319-06590-8_87.
17. **Wang, L. P.; Qiao, G.; Zheng, T. S.** 2008. Analysis and Calculate Model for the Complete Dynamical Coefficients of Tilting-Pad Bearings, Chinese Journal of Mechanical Engineering 44(1): 75-80.
18. **Yang, Q. J.; Li, W. G.; Guo, M. J.; ZHAO, X.; Li, D.** 2021. Research on Initial Working Mechanism of Fluid Pivot Floating Bearing and Floating Characteristics of Single Bottom Pad Bearing, Chinese Journal of Mechanical Engineering 57(7): 125-137. https://doi.org/10.3901/JME.2021.07.125.

19. **Zhang, Z. S.; Dai, X. D.** 2011. Research on the Complete Dynamical Model of Tilting-Pad Bearings Considering the Coupling Moving of Shaft and Pads with Turbulent Oil Film, Advanced Materials Research 338: 611-617. https://doi.org/10.4028/www.scientific.net/AMR.338.611.
20. **Barrett, L. E.; Allaire, P. E.; Wilson, B. E.** 1988. The Eigenvalue Dependence of Reduced Tilting Pad Bearing Stiffness and Damping Coefficients, Tribology Transactions 31(4): 411-419. https://doi.org/10.1080/10402008808981842.
21. **Yan, Z.; Wang, L.; Qiao, G.; Zheng, T.** 2010. An analytical model for complete dynamical coefficients of a tilting-pad journal bearing, Tribology International 43(1-2): 7-15. https://doi.org/10.1016/j.triboint.2009.03.010.
22. **Suh, J.; Palazzolo, A.** 2015. Three-Dimensional Dynamic Model of TEHD Tilting-Pad Journal Bearing—Part I: Theoretical Modeling, ASME Journal of Tribology 137(4): 041703. https://doi.org/10.1115/1.4030020.
23. **Yan, Z.; Lu, Y.; Zheng, T.** 2011. An Analytical Complete Model of Tilting-Pad Journal Bearing Considering Pivot Stiffness and Damping, ASME Journal of Tribology 133(1): 011702. https://doi.org/10.1115/1.4002070.

X. Song, Y. Dong, T. Bai, J. Yu

CALCULATION METHOD OF COMPLETE DYNAMIC CHARACTERISTICS COEFFICIENTS FOR TILTING PAD BEARINGS

S u m m a r y

As energy equipment advances towards higher speeds and greater capacities, the issue of instability in tilting pad bearings has correspondingly grown more pronounced. The method of eight-coefficients dynamic characteristics of the tilting pad bearing exposes many shortcomings. This paper introduces the geometric interplay between the tilting pad bearing and journal movement, advancing a novel method for calculating the comprehensive characteristic coefficients of the bearing, grounded in the concept of tile motion equivalence. According to the geometric relationship between tilting pad bearing and journal movement, the coordinate system of the tilting pad bearing pad performance is established. The motion of the pad is equivalent to the movement of the journal to solve the complete characteristic coefficient, and the relationship between the complete kinetic coefficients is deduced. In contrast to the tile perturbation approach, our method alleviates the complexities associated with determining the complete characteristic coefficients, streamlines the computational workflow, boasts high efficiency and reliability, and is more readily embraced and comprehended by engineering professionals. It provides the support for the calculation of the tilting pad bearing-rotor system stability.

Keywords: tilting pad bearing, complete kinetic coefficient, motion equivalent, dynamic characteristics coefficients.

Received July 20, 2024
Accepted December 16, 2024